Journal of Nuclear Materials 386–388 (2009) 1074–1077

Contents lists available at ScienceDirect

Journal of Nuclear Materials

journal homepage: www.elsevier.com/locate/jnucmat

Study on damage process and hydrogen effect in Li_2ZrO_3 by using ion-induced luminescence

Hirokazu Katsui *, Shinji Nagata, Kentaro Toh, Bun Tsuchiya, Tatsuo Shikama

Institute for Materials Research, Tohoku University, 2-1-1, Katahira, Aoba-ku, Sendai 980-8577, Japan

A B S T R A C T

Ion-beam analysis techniques were employed to examine a dynamic damage process and the relation between hydrogen and oxygen deficiencies in lithium zirconate (Li_2ZrO_3). Ion-induced luminescence was measured under irradiation of protons and helium ions in the energy range of 0.2–2 MeV. The luminescent intensity at around 2.9 eV was proportional to the projected range of incident ions, independent of the electronic energy loss. During ion irradiation, the luminescent intensity monotonically decreased with increasing fluence. This decrease could be explained by a simple model that included annihilation and production processes based on nuclear collisions. At room temperature, hydrogen atoms were uniformly distributed in samples with a maximum concentration of 15 at.%. The samples with a higher hydrogen concentration exhibited a lower luminescent intensity; this suggested that hydrogen trapping was related to the luminescent centers in Li_2ZrO_3.

1. Introduction

Lithium zirconate (Li_2ZrO_3) is of interest for its use in fusion reactor blanket systems as a solid breeding material because of its excellent tritium release behavior especially at low temperatures [1,2]. It is important to clarify the damage process induced by high-energy particles (such as neutrons, alpha-particles, and tritons) and the behavior of hydrogen isotopes in solid breeding materials. By using electron spin resonance (ESR), thermal desorption spectroscopy (TDS) and optical absorption measurements, researchers have indicated that the oxygen vacancy formed by neutron irradiation acts as a tritium trapping site [3–5]. Ion-induced luminescence measurements have been carried out to probe the defects and the impurities in ceramic materials [6,7]. In the case of solid breeding materials, the production behavior of irradiation defects has been discussed by in-situ measurements of the ion-induced luminescence in lithium-containing ceramics [8–10]. Simultaneous measurements of luminescence and tritium release have been carried out in order to investigate the influence of radiation defects on tritium recovery in Li_2O [11]. Among the solid breeding materials, Li_2ZrO_3 exhibits the prominent ion-induced luminescence in the ultraviolet region. Because this luminescence is considered to originate from oxygen vacancies [10], it can be utilized to an investigated the dynamic damage process during ion irradiation.

In this study, we investigated the dynamic changes in luminescence when Li_2ZrO_3 was irradiated with MeV-energy protons and helium ions. In addition, we simultaneously measured the ion-induced luminescence measurements and the hydrogen concentration in order to examine the interaction between hydrogen and oxygen deficiencies in Li_2ZrO_3.

2. Experimental

Li_2ZrO_3 sintered discs with a diameter of 3 or 8 mm and a thickness of 1 mm (TYK Corporation) were used as samples in this study. The X-ray diffraction pattern of the samples revealed a monoclinic crystal structure. The as-received samples included approximately 3 at.% of hydrogen and 0.2 at.% of hafnium. Prior to the measurements of ion-induced luminescence, samples were polished by a sheet of emery paper in order to remove the accumulated hydrogen at the surface layer. Irradiation with protons and helium ions was carried out in a vacuum chamber with a pressure of 10^{-5} Pa at room temperature, using a 1.7-MV tandem accelerator, Institute for Materials Research, Tohoku University. The typical incident ion flux density was 1×10^{16} ions/m^2/s and the maximum fluence, 2×10^{19} ions/m^2 in the incident energy range of 0.2–2 MeV. Ion-induced luminescence was measured through an optical window by using a monochrometer (Acton Research Sp-2356) equipped with a CCD camera (Roper Scientific PIXE100). As the detected luminescent yield was proportional to the incident ion flux, we hereafter define the luminescent intensity as the detected luminescent yield normalized by the incident ion flux. For the depth profiling of hydrogen concentration in the near-surface

* Corresponding author. Tel.: +81 22 215 2063; fax: +81 22 215 2061.
E-mail address: hirokazu829@imr.tohoku.ac.jp (H. Katsui).

0022-3115/$ - see front matter © 2008 Elsevier B.V. All rights reserved.
doi:10.1016/j.jnucmat.2008.12.285

layer, elastic recoil detection analysis (ERDA) was carried out using a 2.8 MeV helium ion-beam. The analyzing beam was irradiated to the sample at the incident angle of 72° to the surface normal, and recoiled hydrogen atoms were detected at an angle of 30° with respect to the analyzing beam by using an Al foil (thickness: 12 μm) to stop the forward-scattered helium ions. Thus, the probing depth of hydrogen was estimated to be approximately 500 nm. In order to investigate the relation between the hydrogen atoms and the ion-induced luminescence, the as-received samples were exposed to humid air for up to 150 h or annealed at 1073 K in air for obtaining samples with various hydrogen concentrations.

3. Results and discussion

3.1. Characteristics of ion-induced luminescence

Fig. 1 shows the luminescent spectra from Li_2ZrO_3 at the beginning of 1-MeV proton and helium ion irradiation. A broad luminescence peak was observed at around 2.9 eV. Although the structure of the luminescent centers is not well understood, it has been considered that the ion-induced luminescence in the ultraviolet region originated from several types of oxygen deficiencies in Li_2ZrO_3 [10]. A photoluminescence spectrum identical to the ion-induced luminescence was also observed by using 5-eV excitation light source. Therefore the initial ion-induced luminescent intensity at the beginning of ion irradiation was attributed to the intrinsic luminescent centers without any damages due to ion bombardments. In Fig. 1, the initial luminescent intensity induced by 1 MeV of protons was approximately three times higher than that induced by 1 MeV of helium ions. Fig. 2 shows the initial luminescence intensity, which was acquired for 1 s from the beginning of the ion irradiation, plotted as a function of the projected range of incident ions calculated by using the SRIM2006 code [12]. The initial luminescence intensity increased with an increase in the projected range of incident ions. Here, due to the optical absorption of the sample, the luminescence intensity attenuated to half at the 10 μm thickness of the sample. In Fig. 2, an inserted curve represents the luminescent intensity including a correction of the optical absorption, on the presumption that the luminescent intensity was proportional to the projected range of incident ions. The result suggested that the ion-induced luminescent intensity was determined by the number of luminescent centers along the trajectory of the incident ions, independent of the electronic energy loss.

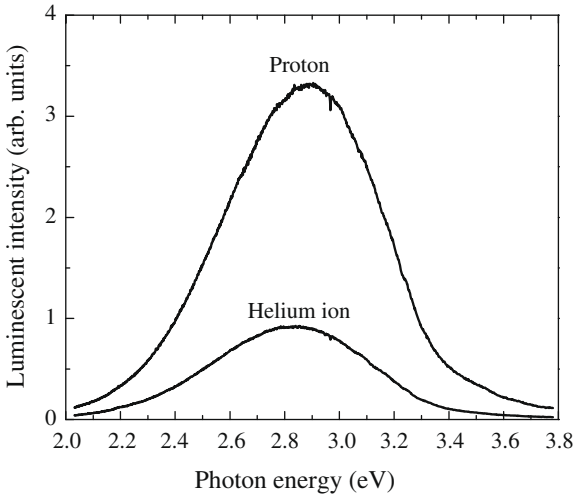

Fig. 1. Initial luminescent spectra from Li_2ZrO_3 under irradiation of 1-MeV protons and helium ions.

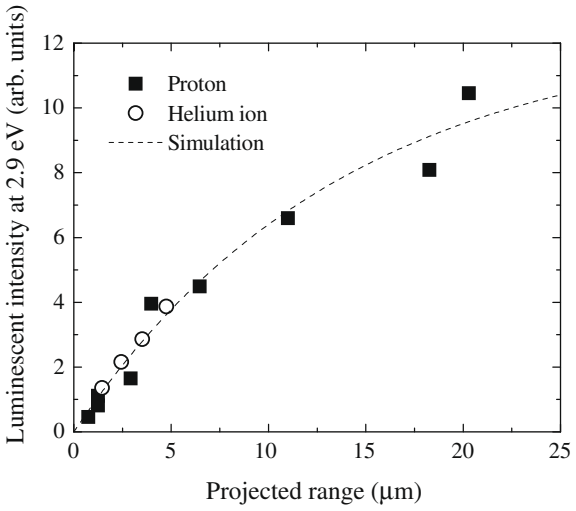

Fig. 2. Initial luminescent intensity at 2.9 eV plotted against the projected range of protons (solid square) and helium ions (open circle) in the energy range of 0.2–2 MeV.

The luminescent efficiency of an incident ion seemed to be constant because the electronic excitation for the luminescent centers along the ion track was saturated by the high electronic energy deposition in Li_2ZrO_3.

3.2. Dynamic damage process under ion irradiation

In order to examine the dynamic damage process, we focused on the changes in the luminescent intensity during ion irradiation by using various incident energies. As seen in Fig. 3, the luminescent intensities monotonically decreased as the fluence of the incident ions increased; the intensities decreased drastically at the beginning of the irradiation, and then, the decreasing rate became smaller with increasing fluence. The decreasing rate under the irradiation of helium ions was larger than that under protons with the same incident energy. The decreasing behavior during the irradiation of protons and helium ions could not be fitted by a first-order reaction model assuming only the annihilation of the luminescent centers with several different rate constants. Meanwhile, the peak

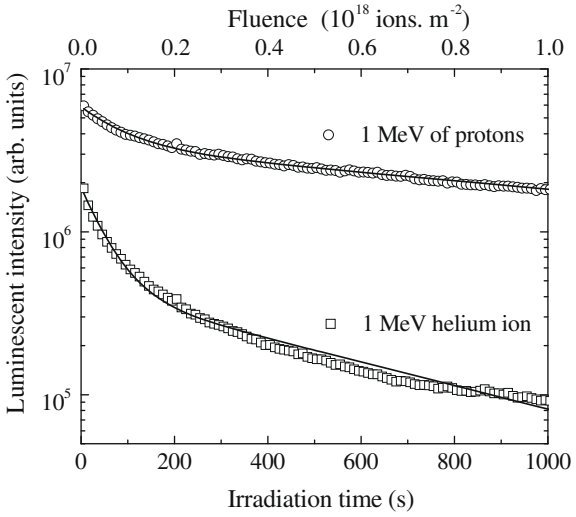

Fig. 3. Luminescent intensity from Li_2ZrO_3 plotted against the irradiation time corresponding to the fluence of 1 MeV protons (circle) and helium ions (square). The solid lines indicate the fitted curves using a model.

shape did not change during the ion irradiation. This suggested that the decrease in luminescent intensity reflected the decrease in the concentration of only one type of the luminescent center. Instead of several annihilation processes of luminescent centers, we introduced a production process in addition to an annihilation of luminescent centers by assuming a precursor that could be converted to a luminescent center by ion bombardment. The differential equations of the production and annihilation processes of the luminescent centers can be described as follows:

$$\frac{dN_P(x,t)}{dt} = -\lambda_1 N_P(x,t) \quad (1)$$

$$\frac{dN_L(x,t)}{dt} = \lambda_1 N_P(x,t) - \lambda_2 N_L(x,t) \quad (2)$$

where $N_L(x, t)$ is the concentration of the luminescent centers at time t and depth x and $N_P(x, t)$, the concentration of the precursors of the luminescent centers. λ_1 and λ_2 are the rate constants of the production from the precursors and the annihilation of the luminescent centers obtained by ion bombardments, respectively. The obtained decreasing curves were fitted by the abovementioned model by using a least-squares method and varying the values of λ_1, λ_2, $N_L(x, 0)$, and $N_P(x, 0)$. The fitted results were inserted in Fig. 3. Fig. 4 shows the values of λ_1 and λ_2 plotted as a function of the nuclear stopping power of the incident ions. It could be clearly observed that both λ_1 and λ_2 increased with increasing nuclear stopping power. In contrast, there seemed to be no apparent correlation between the rate constants and the electronic stopping power. Therefore, the production and the annihilation of the luminescent centers were predominantly attributed to the nuclear collisions and not to the electronic excitation of the incident ions.

3.3. Hydrogen effect on the luminescent intensity

Fig. 5 shows the depth profiles of hydrogen concentration in the near-surface layer of the sample exposed to humid air for 100 h, in comparison with the as-received sample. Initially, the hydrogen concentration was uniform in both the samples; however, the concentration in the former sample increased after the air exposure. In contrast, the ion-induced luminescent intensity of this sample decreased after the air exposure. During the air exposure, hydrogen atoms were introduced into the sample by a dissociation of water vapor at the surface, and then the hydrogen was trapped around an oxygen deficiency. Fig. 6 shows the ion-induced luminescence intensities plotted against the hydrogen concentration in several samples in order to examine the interaction between the hydrogen and the luminescent centers in Li_2ZrO_3. A lower luminescent intensity was obtained for a sample with a higher hydrogen concentration. This result implied that a luminescent center could be transformed into a nonluminescent one by trapping hydrogen around it. Further investigation is required in order to clarify the relation between hydrogen trapping and the luminescent centers in Li_2ZrO_3.

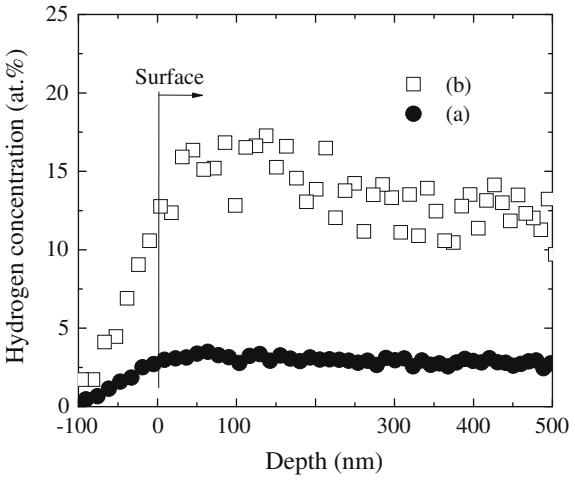

Fig. 5. Depth profiles of hydrogen concentration for the as-received sample (a) and the sample exposed to air for 100 h (b).

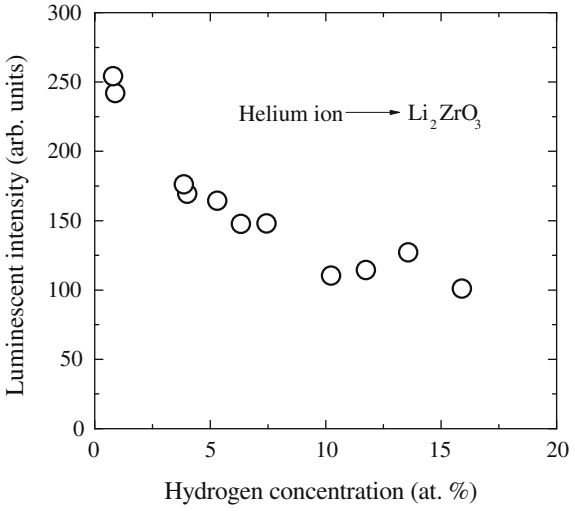

Fig. 6. Luminescent intensity plotted against the hydrogen concentration in Li_2ZrO_3 samples.

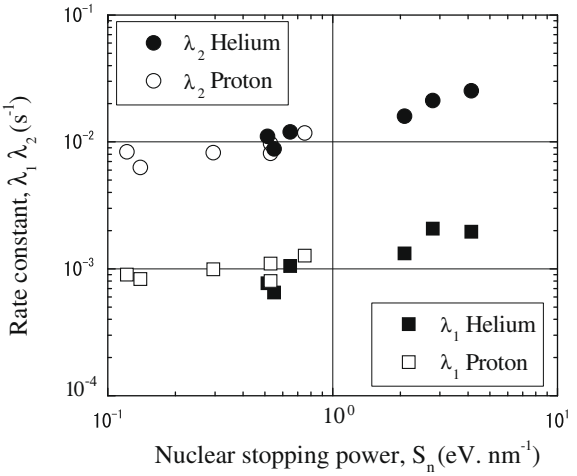

Fig. 4. Rate constants of production (λ_1, square) and annihilation (λ_2, circle) of the luminescent centers plotted against the nuclear stopping power of protons (open) and helium ions (solid) calculated using the SRIM2006 code [12].

4. Conclusion

The ion-induced luminescence at around 2.9 eV from Li_2ZrO_3 was investigated with respect to the dynamic damage processes by ion bombardments and to the relation between the hydrogen and the luminescent centers in Li_2ZrO_3. The ion-induced luminescent intensities were proportional to the number of luminescent centers along the trajectory of the incident ions. The decrease in the luminescent intensity during ion irradiation was well explained by a simple model including annihilation and production

of the luminescent centers. By evaluating the rate constants, we concluded that the nuclear collisions played an important role in both the annihilation and the production of the luminescent centers under ion irradiation. Simultaneous measurements of ion-induced luminescence and hydrogen concentration revealed that a sample with a higher hydrogen concentration exhibited a lower luminescent intensity. It is speculated that a luminescent center could be deactivated by hydrogen trapping.

Acknowledgement

The authors would like to express their sincere gratitude to Dr. Koji Katahira in TYK Corporation for the preparation of the samples. This work was supported by Grant-in-Aid for JSPS Fellows No. 70-7118 from Japan Society for the Promotion of Science (JSPS).

References

[1] N. Roux, J. Avon, A. Floreancig, J. Mougin, B. Rasneur, S. Ravel, J. Nucl. Mater. 233–237 (1996) 1431.
[2] C.E. Johnson, J. Nucl. Mater. 270 (1999) 212.
[3] K. Okuno, H. Kudo, J. Nucl. Mater. 138 (1986) 31.
[4] M. Oyaidzu, H. Kimura, A. Yoshikawa, Y. Nishikawa, K. Munakata, M. Okada, M. Nishikawa, K. Okuno, Fus. Eng. Des. 81 (2006) 583.
[5] K. Noda, K. Uchida, T. Tanifuji, S. Nasu, Phys. Rev. B24 (1981) 3736.
[6] P.W. Haycock, P.D. Townsend, J. Phys. C: Solid State Phys. 20 (1987) 319.
[7] A.A. Finch, J. Garcia-Guinea, D.E. Hole, P.D. Townsend, J.M. Hanchar, J. Phys. D: Appl. Phys. 37 (2004) 2795.
[8] Y. Asaoka, H. Moriyama, K. Iwasaki, K. Moritani, Y. Ito, J. Nucl. Mater. 183 (1991) 174.
[9] K. Moritani, I. Takagi, H. Moriyama, J. Nucl. Mater. 326 (2004) 106.
[10] H. Moriyama, S. Tanaka, K. Noda, J. Nucl. Mater. 258–263 (1998) 587.
[11] V. Grishmanov, S. Tanaka, J. Tiliks, G. Kizane, A. Supe, T. Yoneoka, Fus. Eng. Des. 39–40 (1998) 685.
[12] J.F. Ziegler, <http://www.srim.org>.